A Bridge – Vehicle Interaction Based Experimental Investigation of Damage Evolution

Vikram Pakrashi[1], Alan O' Connor[2] and Biswajit Basu[3]

[1] Postdoctoral Research Fellow, Department of Civil, Structural and Environmental Engineering, Trinity College Dublin, Dublin 2, Ireland. E-mail: pakrashv@tcd.ie

[2] Lecturer, Department of Civil, Structural and Environmental Engineering, Trinity College Dublin, Dublin 2, Ireland. E-mail (corresponding author): alan.oconnor@tcd.ie

Phone: +353 1 896 1822 Fax: +353 1 677 3072

[3] Professor, Department of Civil, Structural and Environmental Engineering, Trinity College Dublin, Dublin 2, Ireland E-mail: basub@tcd.ie

Abstract: This paper presents an experimental monitoring of the evolution of a crack in a beam using the beam-vehicle interaction response signals for identification of progressively increasing crack depth ratios. The beam is traversed by a two-axle model vehicle providing excitation in the time domain for the various extents of damage. The response of the beam in the time domain during the period of forced vibration is measured using strain gauges. A consistent evolution of damage has been demonstrated in terms of the maxima values of the measured responses. Corresponding distortions of wavelet coefficients of the measured strain data due to the presence of various levels of damage have been identified. The evolution of the phase space and the wavelet transformed phase spaces have been evaluated with damage evolution. The wavelet

transformed phase spaces for the undamaged and the damaged cases are observed to be distinctly different at high scales. The importance of denoising of the acquired data and the importance of vehicle configuration have been illustrated. This study presents a basis for a general model free damage assessment and structural health monitoring framework. The presented study is particularly useful in the context of continuous online bridge health monitoring since the data necessary for analysis can be obtained from the operating condition of the bridge and the structure does not need be closed down.

Key Words: Wavelet Coefficient Maps, Distorted Ridges and Skeletons, Wavelet Transformed Phase Space, Damage Evolution, Bridge –Vehicle Interaction

---

1 INTRODUCTION

The possibility of the use of bridge vehicle interaction data for structural health monitoring has gained considerable interest in recent times. A significant amount of literature of varying complexity and detail (both theoretical and experimental) is available on the bridge vehicle interaction process [1, 2, 3, 4, 5] and much of which deals with vehicle and axle identification problems [6, 7, 8, 9], there is a gap in the literature regarding how such data can be used best in structural health monitoring.

Majumdar and Manohar [10] have considered a bridge system with partially immobile bearings and have identified the loss of local stiffness by proposing a time domain damage descriptor. Lee et.al [11] have experimentally investigated the possible

application of bridge-vehicle interaction data for identifying the loss of bending rigidity by continuously monitoring the operational modal parameters. Law and Zhu [12] have considered a simply supported beam with open and breathing cracks and discussed the dynamic behaviour of the bridge-vehicle interaction both from theory and experiment. The phase space was seen to be distorted as compared with an undamaged phase space in their study due to the presence of the crack. A number of studies [13, 14, 15, 16, 17] not related to the bridge-vehicle interaction problem have also observed that the geometry of phase space changes due to the presence of damage in the form of a crack. Bilello et.al [18] and Bilello and Bergman [19] have considered the passage of a moving mass over a damaged beam both theoretically and experimentally. Bu et.al [20] have presented a numerical study for bridge condition assessment from dynamic response of a passing vehicle considering different vehicle models, vehicle speed, sampling frequency, vehicle and bridge mass and stiffness ratios, road surface roughness, measurement noise and model error. Zhu and Law [21] have provided similar numerical studies emphasizing the importance of bridge-vehicle interaction based damage detection in concrete bridges.

These studies consistently relate to the detection, identification of the location of damage and its calibration in the presence of noise, which are the key factors affecting structural health monitoring and maintenance programmes. Such assessment, monitoring and possible predictions of damage evolution have usually been based on the analyses of the spatial or temporal response of a structure and the damage is generally quantified against a pre-existing benchmark [22]. The traditional descriptors of damage, like the change in natural frequencies are often quite small, not robust in the presence of measurement noise and fail to identify the location of damage.

The advent of sophisticated laser based devices [23, 24, 25] and the recent use of comparatively less expensive and accessible digital camera based methods [26, 27, 28, 29] in conjunction with intelligent image processing techniques and wavelet based identification of the presence, location and the extent of damage using spatial data have been reported and have gained considerable interest [30]. While these experimental studies deal with the identification of the location of damage comparatively well, very few of them investigate the evolution of the extent of damage [24, 29]. A large number of studies have been devoted to the problem of an open crack in a simply supported beam [22, 31] in this respect and the use of wavelet analysis on the damaged modeshapes [23] or static deflected shapes [28] has successfully illustrated the potential of wavelet based analyses in identifying damage without a pre-existing benchmark. The main challenge for a damage extent calibration using spatial data however lies in the difficulty of obtaining reliable and appropriate measurements in the presence of noise due to the potentially devastating masking effect [32] where the damage is overridden by the aforementioned measurement noise.

As a result, damage identification techniques in the time domain are still more popular since the data obtained is of comparatively superior quality and the measurements are generally more accessible and comparatively less complicated than obtaining data from the spatial domain. The major studies on damage identification and calibration of beams using temporal data have mostly dealt with the observation of the changes in natural frequency due to the presence of damage [33, 34, 35, 36, 37, 38] , propagation of elastic waves [39, 40], tracking of frequency contours from different modes [41] and local attractor based detections using stochastic and chaotic excitation

where the structure is considered as a filter and the damage is described through phase space reconstruction [42, 43, 44, 45, 46].

All these studies are based either on free vibration or on some external forced vibration, which requires the closure of the structure especially in the case of a bridge. Thus, there exists a necessity to acquire vibration data from the bridge in its operating condition and consequently propose a practical structural health monitoring technique. It is considered that a general model – free damage detection and evolution tracking methodology has a definite potential in structural health monitoring and assessment of bridge structures under operating conditions and in the presence of measurement noise. Since small scale laboratory based experiments can be related to larger prototypes [19, 18], such experiments serve as an efficient and economic way of investigating damage evolution in bridge structures. This motivates the authors to carry out an experiment to track the evolution of damage in a model simply supported damaged beam traversed by a model two-axle vehicle. Damage is simulated in the beam by progressively increasing the extent of an open crack. Strain data at multiple locations have been acquired in the time domain during the forced vibration period. The gradual evolution has been noted first through maxima values of the measured responses at the strain gauges. Distortions of wavelet coefficients of the measured strain data due to the presence of various levels of damage have been observed. The evolution of the phase space and the wavelet transformed phase spaces have been tracked along with the evolution of damage. The importance of denoising of the acquired data and the importance of vehicle configuration have been demonstrated. This study creates a framework for a general model free damage assessment and structural health monitoring which is robust against noise. Since the

analysis is carried out at a signal level, the proposed approach is not limited to linear systems. The study is particularly useful in the context of continuous online bridge health monitoring since the data necessary for analysis can be obtained from the operating condition of the bridge and the structure does not therefore need be closed down.

2 DISCUSSION ON DAMAGE MODELS

Several models exist for an open crack in an Euler Bernoulli beam involving different degrees of complexity. The strain and stress are considered to be maximum at the crack tip and their decay is inversely proportional to the radial distance from the tip. Bovsunovsky and Matveev [47] have modelled a crack as a local reduction of the moment of inertia over an affected width. More complex, accurate and computationally demanding continuous open crack models have been provided by Christides and Barr [48], Shen and Pierre [49] and Carneiro and Inman [50] derived from the stationarity conditions of the Hu-Washizu-Barr functional. These formulations model the local perturbation of strain and displacement fields due to the presence of a crack. A more popular and computationally inexpensive lumped crack model preserving the physical nature of damage has been used by many researchers [22, 24, 51, 39, 52, 31]. The effects of the crack in this formulation are assumed to be present around the immediate neighbourhood of the damage. The lumped crack model is chosen in this paper for the purpose of illustration, although the conclusions and findings are general and not limited by this model. The beam with an open crack is modelled as two uncracked beams connected through a rotational spring at the location of crack. Figure 1 demonstrates that the length of the beam is L with the damage located at a distance of ‘a’ from the left hand

support of the beam. The crack depth is taken as 'c' and the overall depth of the beam is 'h'. The governing free vibration equation is

$$EI\frac{\partial^4 y}{\partial x^4}+\rho A\frac{\partial^2 y}{\partial t^2}=0 \tag{1}$$

where E, I, A and ρ are the Young's modulus, the moment of inertia, the cross sectional area and the density of the material of the beam on either side of the crack. The displacement of the beam from its static equilibrium position is y(x,t), at a distance of x from the left hand support along the length of the beam at any time t. Continuity in displacement, moment and shear are assumed at the location of crack. A slope discontinuity present in the modeshape Φ at the location of the crack and is modelled as

$$\Phi_R'(a)-\Phi_L'(a)=\theta L\Phi_R''(a) \tag{2}$$

where the term θ is the non-dimensional crack section flexibility dependent on the crack depth ratio (CDR) δ(=c/h) and the subscripts R and L denote the right and the left hand side of the damage respectively. As per Narkis [22], the term θ is considered to be a polynomial of δ as

$$\theta=6\pi\delta^2(h/L)(0.5033-0.9022\delta+3.412\delta^2-3.181\delta^3+5.793\delta^4) \tag{3}$$

3 DAMAGED BEAM –MOVING LOAD INTERACTION

The bridge vehicle interaction can be modelled as a beam-moving load interaction process when the primary interest is to find an approximate nature of such interaction and the effects of the interaction on the vehicle are not important [12]. We consider a simply supported Bernoulli Euler beam with an open crack being acted on simultaneously by n number of concentrated loads P_i (i from 1 to n) moving with an initial velocity u_0 and a

constant acceleration f (Figure 1). The forced vibration equation of the problem of the damaged beam is

$$EI\frac{\partial^4 y(x,t)}{\partial x^4}+\hat{c}\frac{\partial y(x,t)}{\partial t}+\rho A\frac{\partial^2 y(x,t)}{\partial t^2}=\sum_{i=1}^{n}P_i\hat{\delta}(x-(u_0t+\frac{1}{2}ft^2)) \quad (4)$$

The term $\hat{c}$ is the coefficient of damping and $\hat{\delta}$ is the Dirac-Delta function. The first fundamental mode of the beam contributes much more than the other higher modes and thus sufficiently accurate results can be obtained considering only the first mode of vibration [53]. Considering the first fundamental mode of the beam, by the method of separation of variables it is obtained.

$$y(x,t)=\Phi(x)q(t) \quad (5)$$

The term q(t) is the temporal response of the beam. Considering the free vibration equation 1, the modeshape $\Phi(x)$ is found to be (Narkis (1994))

$$\Phi_L=C_{1L}Sin(\lambda x)+C_{2L}Cos(\lambda x)+C_{3L}Sinh(\lambda x)+C_{4L}Cosh(\lambda x) \qquad 0\le x<a \quad (6.1)$$

and

$$\Phi_R=C_{1R}Sin(\lambda x)+C_{2R}Cos(\lambda x)+C_{3R}Sinh(\lambda x)+C_{4R}Cosh(\lambda x) \qquad a\le x\le L \quad (6.2)$$

for the sub-beams on the left and the right side of the rotational spring respectively. The terms $C_{(.)}$ are integration constants arising from the solution of the separated fourth order differential equation in space. The term λ is expressed as

$$\lambda=(\frac{\rho A\omega^2}{EI})^{1/4} \quad (7)$$

where the natural frequency of the cracked beam is ω. By substituting equation 5 in equation 4, multiplying both sides by $\Phi(x)$, integrating over the length and rearranging, gives

$$\ddot{q}(t) + 2\xi\omega\dot{q}(t) + \omega^2 q(t) = \sum_{i=1}^{n} \frac{P_i}{\rho A \widehat{K}} \Phi(u_0 t + \frac{1}{2} f t^2) \tag{8}$$

because of the sampling property of Dirac Delta function. The term ξ denotes the damping ratio of the beam and the factor $\widehat{K}$ is given as

$$\widehat{K} = \int_0^L \Phi(x).\Phi(x)dx \tag{9}$$

The term D_{ij} is defined as

$$D_{ij(.)} = \frac{P_i C_{j(.)}}{\rho A K} \tag{10}$$

where the subscripts L and R are appended within the parentheses depending on the location of the moving load with respect to the location of damage. The force of excitation F(t) is thus expressed as

$$\begin{aligned} F(t) = {} & D_{i1(.)} Sin\lambda(u_0 t + \frac{1}{2} f t^2) + D_{i2(.)} Cos\lambda(u_0 t + \frac{1}{2} f t^2) + D_{i3(.)} Sinh\lambda(u_0 t + \frac{1}{2} f t^2) \\ & + D_{i4(.)} Cosh\lambda(u_0 t + \frac{1}{2} f t^2) \end{aligned} \tag{11}$$

The second order differential equation 8 in the time domain can be solved in closed form when the velocity of the vehicle is constant (f = 0) by choosing the solution to be

$$q(t) = G_{i1(.)} Sin\lambda(u_0 t) + G_{i2(.)} Cos\lambda(u_0 t) + G_{i3(.)} Sinh\lambda(u_0 t) + G_{i4(.)} Cosh\lambda(u_0 t) \tag{12}$$

Substituting equation 12 in equation 8 and equating the coefficients of the trigonometric terms, gives a set of linear equations as

$$\begin{bmatrix} \omega^2-\lambda^2u_0^2 & -2\xi\omega\lambda u_0 & 0 & 0 \\ 2\xi\omega\lambda u_0 & \omega^2-\lambda^2u_0^2 & 0 & 0 \\ 0 & 0 & \omega^2+\lambda^2u_0^2 & 2\xi\omega\lambda u_0 \\ 0 & 0 & 2\xi\omega\lambda u_0 & \omega^2+\lambda^2u_0^2 \end{bmatrix} \begin{Bmatrix} G_{i1(.)} \\ G_{i2(.)} \\ G_{i3(.)} \\ G_{i4(.)} \end{Bmatrix} = \begin{Bmatrix} D_{i1(.)} \\ D_{i2(.)} \\ D_{i3(.)} \\ D_{i4(.)} \end{Bmatrix} \tag{13}$$

The terms $G_{ij(.)}$ are solved as

$$G_{i1(.)} = \frac{(\omega^2-\lambda^2u_0^2)D_{i1(.)} + (2\xi\omega\lambda u_0)D_{i2(.)}}{(\omega^2-\lambda^2u_0^2)^2 + (2\xi\omega\lambda u_0)^2} \tag{14.1}$$

$$G_{i2(.)} = \frac{-(2\xi\omega\lambda u_0)D_{i1(.)} + (\omega^2-\lambda^2u_0^2)D_{i2(.)}}{(\omega^2-\lambda^2u_0^2)^2 + (2\xi\omega\lambda u_0)^2} \tag{14.2}$$

$$G_{i3(.)} = \frac{(\omega^2+\lambda^2u_0^2)D_{i3(.)} - (2\xi\omega\lambda u_0)D_{i4(.)}}{(\omega^2+\lambda^2u_0^2)^2 - (2\xi\omega\lambda u_0)^2} \tag{14.3}$$

$$G_{i4(.)} = \frac{-(2\xi\omega\lambda u_0)D_{i3(.)} + (\omega^2+\lambda^2u_0^2)D_{i4(.)}}{(\omega^2+\lambda^2u_0^2)^2 - (2\xi\omega\lambda u_0)^2} \tag{14.4}$$

The closed form solution of the problem with an accelerating vehicle is extremely cumbersome and laborious. The solution of the interaction process considering vehicle acceleration has thus been performed using numerical methods by converting the equation in its state space form as a system of ordinary linear differential equations and integrating using the $4/5^{th}$ order Runga-Kutta method. The matrix formulation of equation 8 is provided in Appendix 1.

It is thus seen that the additional terms (Cos, Sinh and Cosh) present in the modeshape translate themselves into the time domain through the interaction with the moving load. The excitation force for successful damage detection requires that the damage effects are tangible in the phase space of the structure. Since the beam-moving force interaction problem preserves the singularities in the space domain and translates them into the time domain as the forcing function, this excitation due to the moving load can be considered to be ideal for a structural health monitoring process. The observation of the evolution of damage in the time domain is thus considered to be of significant interest.

4 WAVELET ANALYSIS

The continuous wavelet transform of a square integrable function f(x) can be represented as

$$Wf(b,s) = \int_{-\infty}^{+\infty} f(x) \frac{1}{\sqrt{s}} \psi^*\left(\frac{x-b}{s}\right) dx \tag{15}$$

where the wavelet basis function $\psi(x)$ is a square integrable zero average function and s and b are the scale and the translation parameters respectively. The asterisk denotes a complex conjugation. The function $\psi(x)$ also ensures a weak admissibility condition in the frequency domain as

$$\int_{0}^{+\infty} \frac{\left|\hat{\psi}(\omega)\right|^2}{\omega} d\omega < +\infty \tag{16}$$

where $\hat{\psi}(\omega)$ is a Fourier domain representation of $\psi(x)$ and ω is denotes the frequency.

5 EXPERIMENTS

5.1 Experimental Setup

To explore the aforementioned proposition, experiments were carried out on a 0.91m long phenolic beam with a model two - axle (axle distance 0.11m) vehicle traversing it. Figure 2 shows the general arrangement of the experiment. An open crack into the lower section of the beam was notched at a distance of 0.46m from the left hand side. The cross section of the beam was 50mm x 12mm. Two strain gauges were located at distances 0.42m (Gauge 1) and 0.52m (Gauge 2) from the left hand support of the beam respectively. The vehicle was attached to a string which in turn could be coiled around a motor. The acceleration of the vehicle could be controlled by increasing the voltage in the motor. Three damage conditions comprising crack depth ratios of 0.167, 0.33 and 0.5 respectively were considered for the beam along with the undamaged condition. The vehicle started from rest on the beam and left the beam via an exit platform. Figure 3 shows the photograph of the arrangement. The response due to the forced vibration is recorded by the strain gauges using a commercial data acquisition software StrainSmart System 6000 [54].

5.2 Wavelet Based Multilevel Denoising

The strain data obtained from the forced vibration of the vehicle traversing the beam was observed to be very noisy. This is usually a typical and a very critical problem for

realistic data acquisition systems which is compounded on real structures. Generally most studies on bridge vehicle interaction and structural health monitoring problems have concentrated on additive Gaussian white noise corrupting the acquired signals and present noise stress tests [11, 10, 20, 21]. Although such studies are very useful, often non-white noise affects the signal and has therefore to be taken into account. The denoising, in such cases can be carried out through a level dependent wavelet based estimation of the corruptive additive noise [55]. This multilevel wavelet based denoising has demonstrated superior performance in the present experiment in preference to a single level estimation of noise based on the first level coefficients on the wavelet transform. Figures 4a and 4b provide representative examples of the two gauges illustrating the efficiency of such denoising technique. The vehicle load and the acceleration were 7.5N and 1.1478 m/s^2 respectively. The strain data were denoised at level 6 using Coif4 wavelet basis function employing minimax algorithm and soft thresholding using the MATLAB wavelet toolbox [55].

5.3 Calibration of Damage through Strain Maxima

Law and Zhu [12] had indicated that the normalized deflections can be a sensitive indicator of the damage conditions. Since the dynamic strain can be mechanically related to the dynamic displacements, the gradual increase of the maxima values of the strain responses at the gauges has been tracked in this experiment to calibrate the correspondingly increasing damage extent. Figures 5a and 5b show the evolution of the strain responses at the two gauges for various damage conditions, while Figures 6a and 6b provide the raw and the normalized calibration values of damage respectively. The

calibrations are found to be consistent. It is observed that such calibration is particularly robust against small variations of residence times of the vehicle on the beam (Figures 5 and 6).

5.4 Distortion of Wavelet Coefficient Maps

Melhem and Kim [56] and Kim and Melhem [57,58] reported experimental results on a concrete beam under fatigue loading and have considered the wavelet transform of the acceleration response of the beam at various damage conditions against an impulse. The ridges and skeletons of the wavelet transform maps were observed to be significantly distorted in the presence of large damages. Figures 7a and 7b in this paper presents the absolute values of the wavelet transform coefficients of the strain data from the beam-vehicle interaction process across a range of scales at the two gauges respectively for the various extents of damage in the beam. Significant distortion in the ridges and skeletons are observed with the increase of damage over a range of scales. A consistent descriptor of such distortion, though non-trivial, can thus be helpful in characterizing the evolution of the extent damage in a structure.

5.5 Damage Evolution Tracking

Law and Zhu [12] have shown before that the phase space of the bridge-vehicle interaction becomes distorted in the presence of damage. As a direct consequence, phase space evolution tracking with increasing damage under controlled conditions of the entry and the exit of a preselected and calibrated vehicle can be helpful in terms of characterizing damage extents and the temporal evolution of a bridge. However, due to

practical limitations of data acquisition or due to the unwanted participation of measurement noises corrupting the signal, it can often be difficult to obtain a meaningful insight directly from the evolution of the phase space. Also, even with sufficiently denoised measurements, a numerical differentiation to obtain velocity data accentuates the small noises still present in the signal, especially for cases when only the displacement or the strain data is available, as is often the case for instrumented structural bridges. A typical situation is presented in Figures 8a and 8b where the microstrain (ε) and its derivative ($\dot{\varepsilon}$) (the strain is directly related to the dynamic displacement) are plotted and the evolution of such plot is tracked for different damage conditions in the two gauges. To get around this difficulty, the authors propose a wavelet transformed phase space tracking for a consistent monitoring of the evolution of damage. The wavelet transformed phase space filters the corrupting noise, smoothes out the signals and retains the relative difference between the damaged and the undamaged cases from a global perspective. The wavelet transformed phase spaces for the undamaged and the damaged cases are observed to be distinctly different at high scales. To illustrate this, Figures 9a to 9g are presented to track the evolution of damage in terms of wavelet transformed phase space formed by the strain and its derivative for the first gauge, i.e. the gauge closest to the damage. The x and the y axes of Figure 9 have been indicated as $W^{(.)}\varepsilon$ and $W^{(.)}\dot{\varepsilon}$ respectively, where the term W stands for the wavelet transform and the number within the superscripted parentheses represents the scale at which the wavelet transform is performed. The phase space tracking is also important from the point of view that such tracking involves the contributions of all of the measured points significantly differing from the undamaged state at a number of scales. The development of a geometric

measure of the distortion of the phase space, though non-trivial, can thus be of great importance when considering the damage model independent generality and the robustness of the approach for the purpose of calibration of damage extent.

6 CONCLUSION

An experimental monitoring of the evolution of an open crack in a beam is presented using a beam-vehicle interaction signal during the forced vibration period for progressively increasing crack depth ratios. A wavelet based multilevel denoising for acquired data corrupted by realistic non-white noise as a preprocessing has been proposed and demonstrated be effective. Damage calibration in terms of the maxima values of the measured responses has been found to be consistent and robust against small variations of the residence time of the vehicle on the beam. The ridges and skeletons of the wavelet coefficient maps of the measured beam-vehicle interaction response have been found to be distorted due to the presence of damage. The robustness (against noise) of tracking the evolution of increasing damage in terms of wavelet transformed phase spaces at higher scales has been demonstrated with the wavelet transformed phase spaces for the damaged cases being distinctly different from the corresponding undamaged ones at high scales. The conclusions are model independent, not limited to linear problems or the problem of bridge-vehicle interaction alone. The study is particularly useful in the context of continuous online bridge health monitoring since the data necessary for analysis can be obtained from the operating condition of the bridge and the structure does not need be closed down.

REFERENCE

1. Abdel –Rohman, M. and Al-Duaij, J. (1996). Dynamic Response of a Hinged-Hinged Single Span Bridges with Uneven Deck. *Computers and Structures*, *59*, 291-299.

2. Delgado, R.M. and S.M. dos Santos, R.C. (1997). Modelling of a Railway Bridge-Vehicle Interaction on High Speed Tracks. *Computers and Structures*, *63*, 511-523.

3. Pesterev, A.V. and Bergman, L.A. (1997). Vibration of Elastic Continuum Carrying Accelerating Oscillator. *ASCE Journal of Engineering Mechanics*, *123(8)*, 886-889.

4. Song, M.K., Noh, H.C. and Choi, C.K. (2003). A New Three Dimensional Finite Element Analysis Model of High-Speed Train-Bridge Interactions. *Engineering Structures*, *25*, 1611-1626.

5. Da Silva, J.G.S. (2004). Dynamical Performance of Highway Bridge Decks with Irregular Pavement Surface. *Computers and Structures*, *82*, 871-881.

6. Law, S.S., Chang T.H.T. and Zeng,Q.H. (1997). Moving Force Identification: A Time Domain Method. *Journal of Sound and Vibration*, *201(1)*, 1-22.

7. Zhu, X,Q. and Law, S.S. (2000). Identification of Vehicle Axle Loads From Bridge Dynamic Responses. *Journal of Sound and Vibration*, *236(4)*, 705-724.

8. Zhu, X.Q. and Law, S.S. (2003). Identification of Moving Interaction Force With Incomplete Velocity Information. *Mechanical Systems and Signal Processing*, *17(6)*, 1349-1366.

9. Jiang, R.J., Au, F.T.K. and Cheung, Y.K. (2004). Identification of Vehicles Moving on Continuous Bridges with Rough Surface. *Journal of Sound and Vibration*, *274(5)*,1045-1063.

10. Majumdar, L. and Manohar C.S. (2003). A Time-Domain Approach for Damage Detection in Beam Structures Using Vibration Data with a Moving Oscillator as an Excitation Source. *Journal of Sound and Vibration*, *268(4)*, 699-716.

11. Lee, J.W., Kim, J.D., Yun, C.B., Yi, J.H. and Shim, J.M. (2002). Health Monitoring Method for Bridges Under Ordinary Traffic Loadings. *Journal of Sound and Vibration*, *257(2)*, 247-264.

12. Law, S.S. and Zhu, X.Q. (2004). Dynamic Behaviour of Damaged Concrete Bridge Structures under Moving Vehicular Loads. *Engineering Structures*, *26(9)*, 1279-1293.

13. Brandon, J.A. and Mathias, A.H. (1995). Complex Oscillatory Behaviour in a Cracked Beam under Sinusoidal Excitation. *Journal of Sound and Vibration*, *186(2)*, 350-354.

14. Brandon J.A. and Abraham O.N.L. (1995). Counter-Intuitive Quasi-Periodic Motion in the Autonomous Vibration of Cracked Timoshenko Beams. *Journal of Sound and Vibration* ,*185(3)*, 415-430.

15. Brandon, J.A. and Sudraud, C. (1998). An Experimental Investigation into the Topological Stability of a Cracked Cantilever Beam. *Journal of Sound and Vibration*, *211(4)*, 555-569.

16. Cheng, S.M., Wu X.J., Wallace, W. and Swamidas, A.S.J. (1999). Vibrational Response of a Beam With a Breathing Crack. *Journal of Sound and Vibration*, *225(1)*, 201-208.

17. Carpinteri, A. and Pugno,N. (2005).Towards Chaos in Vibrating Damaged Structures-Part II: Parametrical Investigation. *ASME Journal of Applied Mechanics*, *72(4)*, 519-526.

18. Bilello, C., Bergman, L.A. and Kuchma, D. (2004). Experimental Investigation of a Small Scale Bridge Model under a Moving Mass. *ASCE Journal of Structural Engineering*, *130(5)*, 799-804.

19. Bilello, C. and Bergman L.A. (2004). Vibration of Damaged Beams under a Moving Mass:Theory and Experimental Validation. *Journal of Sound and Vibration*, 274, 567-582.

20. Bu, J.Q., Law, S.S. and Zhu, X.Q. (2006). Innovative Bridge Condition Assessment from Dynamic Response of a Passing Vehicle. *ASCE Journal of Engineering Mechanics*, *132(12)*, 1372-1379.

21. Zhu, X.Q. and Law, S.S. (2007). Damage Detection in Simply Supported Concrete Bridge Structures under Moving Vehicular Loads. *ASME Journal of Vibration and Acoustics*, *129(2)*, 58-65.

22. Narkis, Y. (1998). Identification of Crack Location in Vibrating Simply Supported Beams. *Journal of Sound and Vibration*, *172(4)*, 549-558.

23. Khan A.Z., Stanbridge A.B. and Ewins, D.J. (2000). Detecting Damage in Vibrating Structures with a Scanning LDV. *Optics and Lasers in Engineering*, *32(1)*, 583-592.

24. Okafor, A.C. and Dutta. A. (2000). Structural Damage Detection in Beams by Wavelet Transforms. *Smart Materials and Structures*, *9(6)*, 906-917.

25. Vanlanduit, S., Guillaume, P., Schoukens, J. and Parloo, E. Linear and Nonlinear Damage Detection Using a Scanning Laser Vibrometer, *Fourth International Conference on Vibration Measurements by Laser Techniques: Advances and Applications*, *SPIE, Vol 4072.*

26. Patsias,S. and Staszewski, W.J. (2002). Damage Detection using Optical Measurements and Wavelets. *Structural Health Monitoring*, *1(1)*, 5-22.

27. Poudel, U.P., Fu, G. and Ye, J. (2005). Structural Damage Detection using Digital Video Imaging Technique and Wavelet Transformation. *Journal of Sound and Vibration*, *286(5)*, 869-895.

28. Rucka, M. and Wilde K. (2006). Crack Identification using Wavelets on Experimental Static Deflection Profiles. *Engineering Structures*, *28(2)*, 279-288.

29. Pakrashi, V., Basu, B. and O' Connor, A. (2007). Structural Damage Detection and Calibration using a Wavelet-Kurtosis Technique. *Engineering Structures*, *29(9)*, 2097–2108.

30. Taha, M.M.R., Noureldin, A., Lucero, J.L. and Baca, T.J. (2006). Wavelet Transform for Structural Health Monitoring: A Compendium of uses and Features. *Structural Health Monitoring*, *5(3)*, 267-295.

31. Lam, H.F., Lee, Y.Y., Sun, H.Y., Cheng, G.F., and Guo,X. (2005). Application of the Spatial Wavelet Transform and Bayesian Approach to the Crack Detection of a Partially Obstructed Beam. *Thin Walled Structures*, *43(1)*, 1-21.

32. Gentile, A. and Messina A. (2003). On the Continuous Wavelet Transforms Applied to Discrete Vibrational Data for Detecting Open Cracks in Damaged Beams. *International Journal of Solids and Structures*, *40(2)*, 295-315.

33. Dado, M.H. (1997). A Comprehensive Crack Identification Algorithm for Beams under Different End Conditions. *Applied Acoustics*, *51 (4)*, 381-398.

34. Chati, M., Rand,R. and Mukherjee, S. (1997). Modal Analysis of a Cracked Beam. *Journal of Sound and Vibration*, *207(2)*, 249-270.

35. Masoud, S., Jarrah, M.A. and Al-Mamoory, M. (1998). Effect of Crack Depth on the Natural Frequency of a Prestressed Fixed-Fixed Beam. *Journal of Sound and Vibration*, *214(2)*, 201-212.

36. Lakshmi Narayana, K. and Jebraj, C. (1999). Sensitivity Analysis of Local/Global Modal Parameters for Identification of Crack in a Beam. *Journal of Sound and Vibration*, *228(5)*, 977-994.

37. Kisa, M. (2004). Free Vibration Analysis of a Cantilever Composite Beam with Multiple Cracks. *Composites Science and Technology*, *64(9)*, 1391-1402.

38. Tomasel, F.G. and Laura, P.A.A. (2002). Assessing the Healing of Mechanical Structures Through Changes in their Vibrational Characteristics as Detected by Fibre Optic Bragg Gratings. *Journal of Sound and Vibration*, *253(2)*, 523-527.

39. Tian, J., Li, Z., and Su, X. (2003), Crack Detection in Beams by Wavelet Analysis of Transient Flexural Waves, *Journal of Sound and Vibration*, *261(4)*, 715-727

40. Wang, X.D. and Huang G.L. (2004). Identification of Embedded Cracks using Back Propagating Elastic Waves. *Inverse Problems*, *20(4)*, 1393-1409.

41. Yang, X.F., Swamidas, A.S.J. and Seshadri, R. (2001). Crack Identification in Vibrating Beams Using the Energy Method. *Journal of Sound and Vibration*, *244(2)*, 339-357.

42. Todd, M.D., Nichols, J.M., Pecora, L.M. and Virgin, L.M. (2001). Vibration Based Damage Assessment Utilizing State Space Geometry Changes: Local Attractor Variance Ratio. *Smart Materials and Structures*, *10(5)*, 1000-1008.

43. Moniz, L., Nichols,J., Trickey,S.,Seaver,M., Pecora,D. and Pecora,L. (2005). Using Chaotic Forcing to Detect Damage in a Structure. *Chaos*, *15, 023106*,1-10.

44. Moniz, M., Nichols, J.M., Nichols, C.J., Seaver, M., Trickey,S.T., Todd, M.D., Pecora, L.M. and Virgin L.M. (2005). A Multivariate, Attractor-Based Approach to Structural Health Monitoring. *Journal of Sound and Vibration*, *283(2)*, 295-310.

45. Nichols, J.M., Todd, M.D. and Seaver, M. (2003). Use of Chaotic Excitation and Attractor Property Analysis in Structural Health Monitoring. *Physical Review E*, *67, 016209*, 1-8.

46. Nichols, J.M., Trickey, S.T., Todd, M.D. and Virgin, L.N. (2003). Structural Health Monitoring Through Chaotic Interrogation. *Meccanica*, *38(2)*, 239-250.

47. Bovsunovsky, A.P. and Matveev, V.V. (2000). Analytical Approach to the Determination of Dynamic Characteristics of a Beam with a Closing Crack. *Journal of Sound and Vibration*, *235(3)*, 415-434.

48. Christides, S. and Barr, A.D.S.(1984). One-dimensional Theory of Cracked Bernoulli-Euler Beams. *International Journal of Mechanical Sciences*, *26(12)*, 639-648.

49. Shen, M.H.H and Pierre, C.(1994). Free Vibration of Beams with a Single Edge Crack. *Journal of Sound and Vibration*, *170(2)*, 237-259.

50. Carneiro, S.H.S and Inman, D.J.(2002). Continuous Model for the Transverse Vibration of Cracked Timoshenko Beams. *ASME Journal of Vibration and Acoustics*, *124(2)*, 310-320.

51. Chang, C.C and Chen, L W. (2003). Vibration Damage Detection of a Timoshenko Beam by Spatial Wavelet Based Approach. *Applied Acoustics*, *64(12)*, 1217-1240

52. Loutridis, S., Douka, E. and Trochidis, A. (2004). Crack Identification in Double Cracked Beams using Wavelet Analysis. *Journal of Sound and Vibration*, *277(5)*, 1025-1039.

53. Yang, Y.B. and Lin C.W. (2005). Vehicle-Bridge Interaction Dynamics and Potential Applications. *Journal of Sound and Vibration*, *284(1)*, 205-226.

54. Vishay Micro-Measurements, *System 5000 StrainSmart Data System*, URL http://www.vishay.com/brands/measurements_group/guide/inst/6000/6000.htm [accessed 2 August 2007].

55. Misiti, M., Misiti, Y., Oppenheim, G. and Poggi, J. M. (2006). Wavelet Toolbox for use with MATLAB. *The Mathworks Inc., 3 Apple Hill Drive, Natick, MA, USA*.

56. Melhem, H. and Kim, H. (2003). Damage Detection in Concrete by Fourier and Wavelet Analysis. *ASCE Journal of Engineering Mechanics*, *129(5)*, 571-577.

57. Kim, H. and Melhem, H. (2003). Fourier and Wavelet Analysis for Fatigue Assessment of Concrete Beams, *Experimental Mechanics*, *43 (2)*, 131-140.

58. Kim, H. and Melhem, H. (2004). Damage Detection of Structures by Wavelet Analysis. *Engineering Structures*, *26(3)*, 347-362.

List of Figures

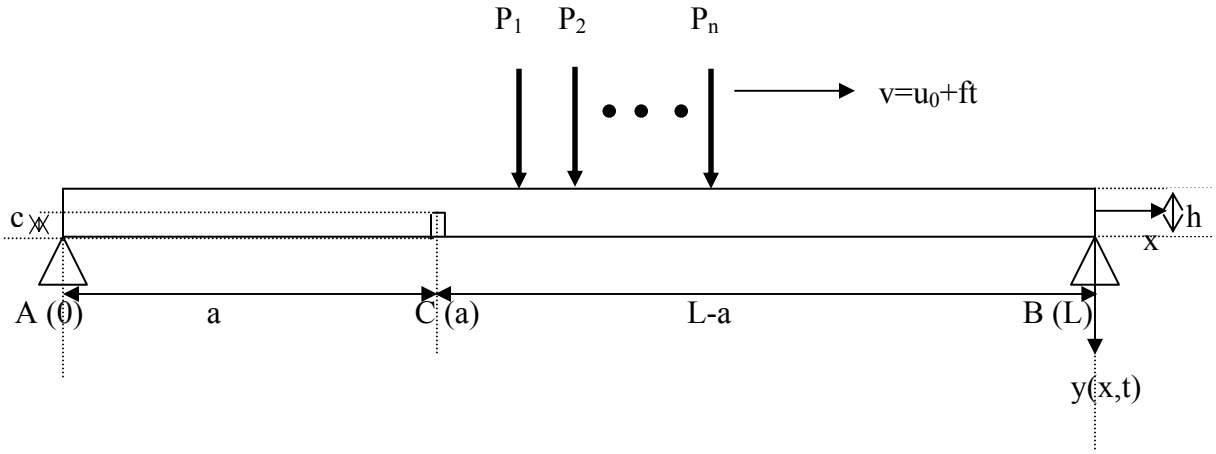

Figure 1.

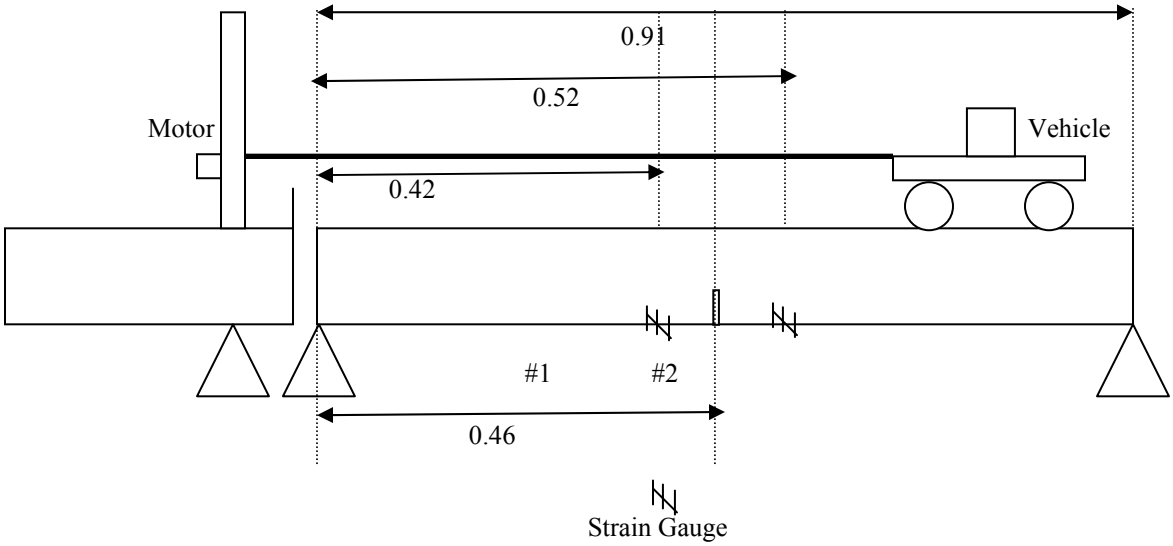

Figure 2.

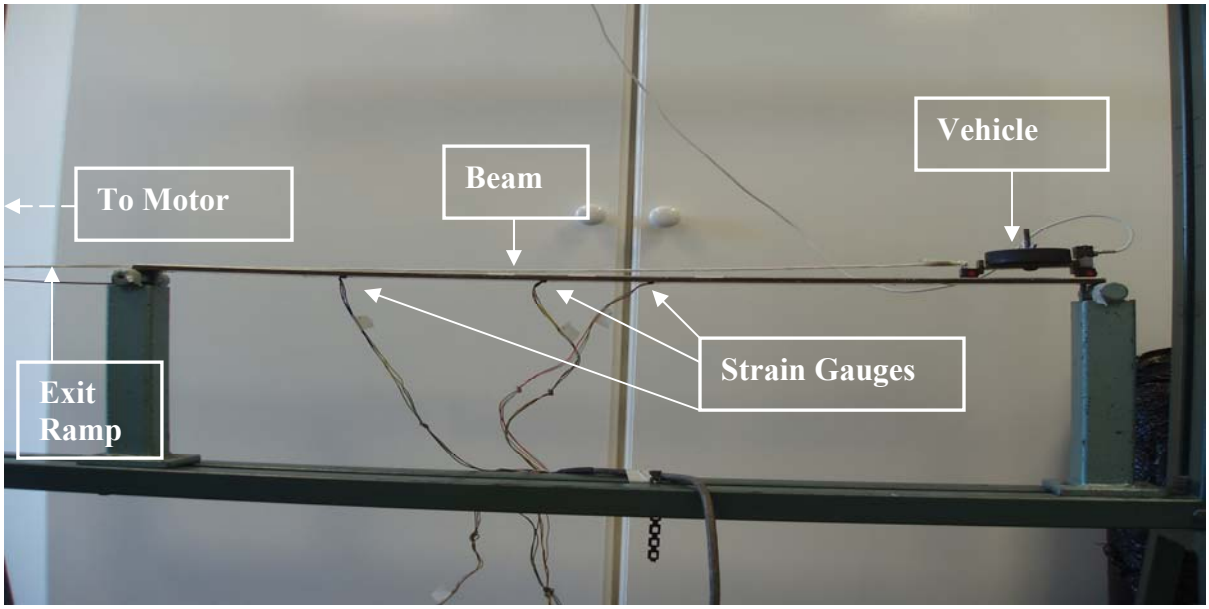

Figure 3.

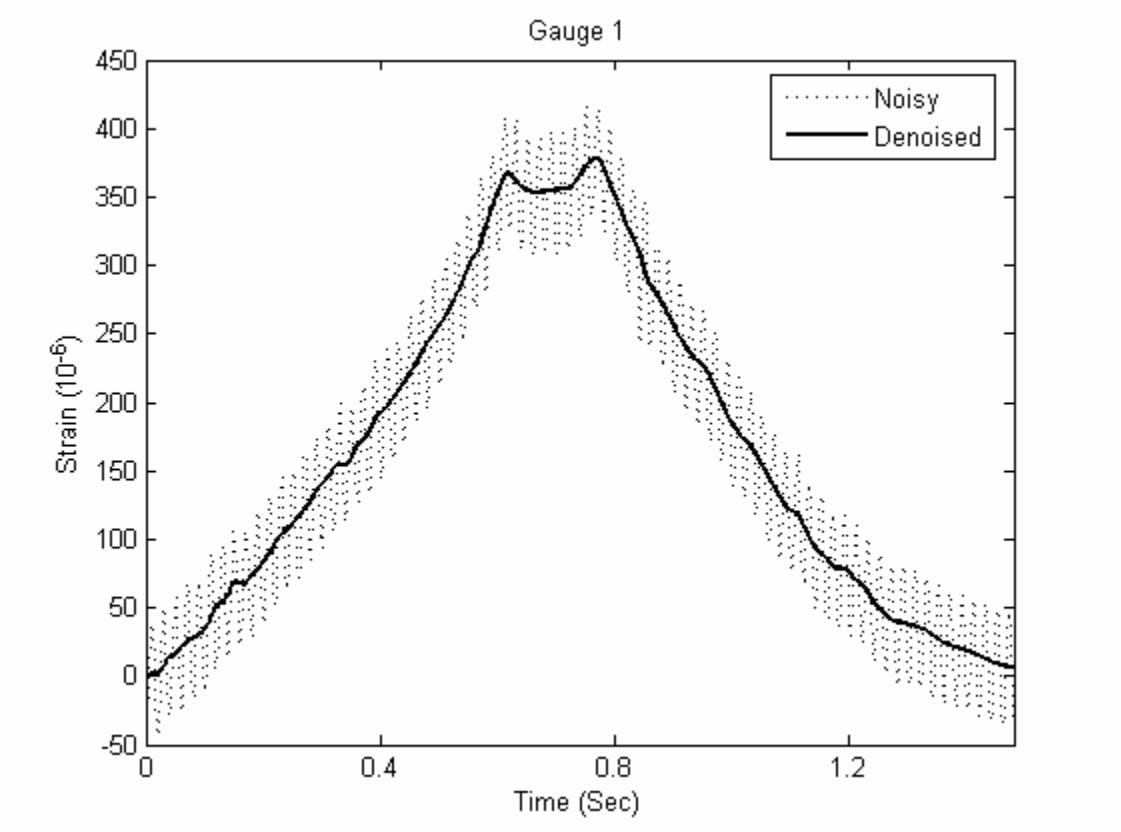
Gauge 1
Noisy
Denoised
Strain (10-6)
Time (Sec)
450
400
350
300
250
200
150
100
50
0
-50
0
0.4
0.8
1.2

Figure 4a.

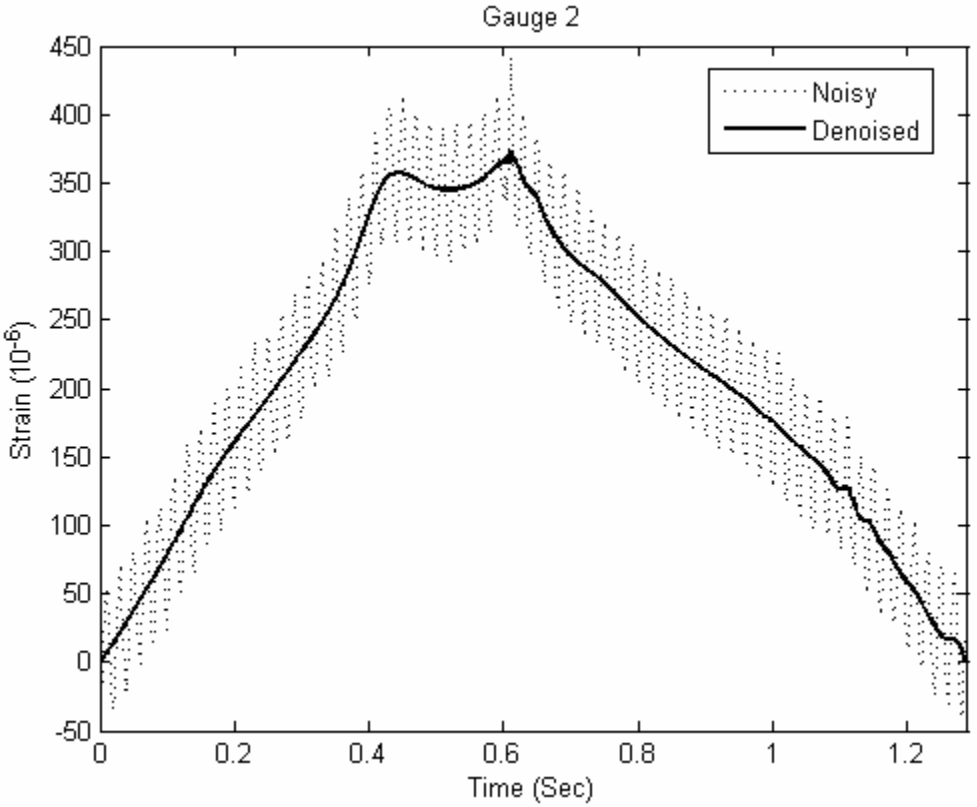
Gauge 2
Noisy
Denoised
Strain (10^{-6})
Time (Sec)
450
400
350
300
250
200
150
100
50
0
-50
0
0.2
0.4
0.6
0.8
1
1.2

Figure 4b.

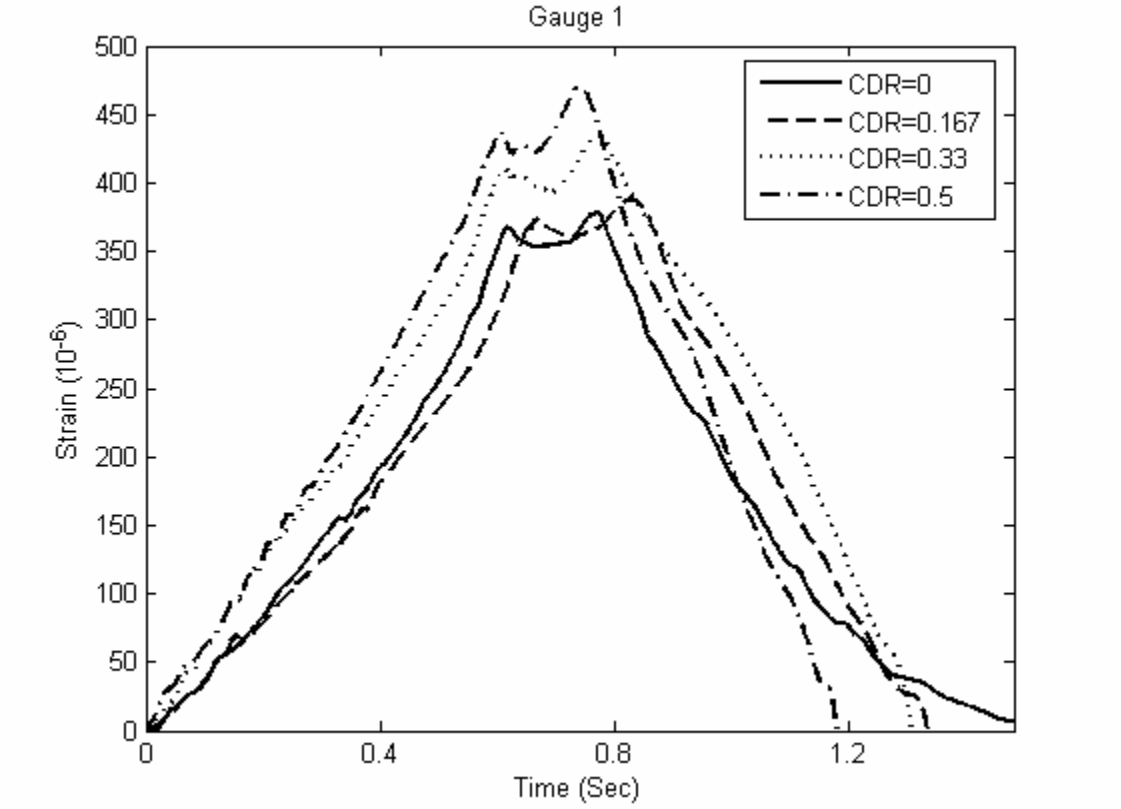
Gauge 1
CDR=0
CDR=0.167
CDR=0.33
CDR=0.5
Strain (10-6)
Time (Sec)
0
50
100
150
200
250
300
350
400
450
500
0
0.4
0.8
1.2

Figure 5a.

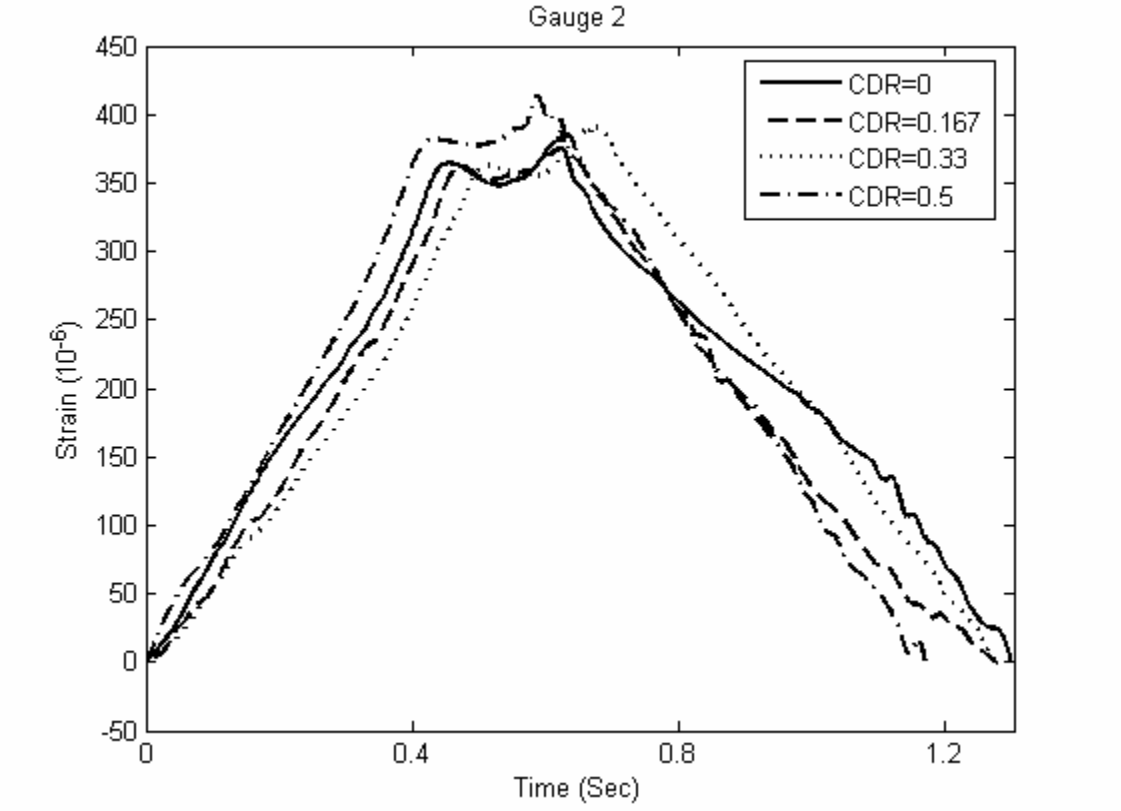
Gauge 2
CDR=0
CDR=0.167
CDR=0.33
CDR=0.5
Strain (10-6)
Time (Sec)
450
400
350
300
250
200
150
100
50
0
-50
0
0.4
0.8
1.2

Figure 5b.

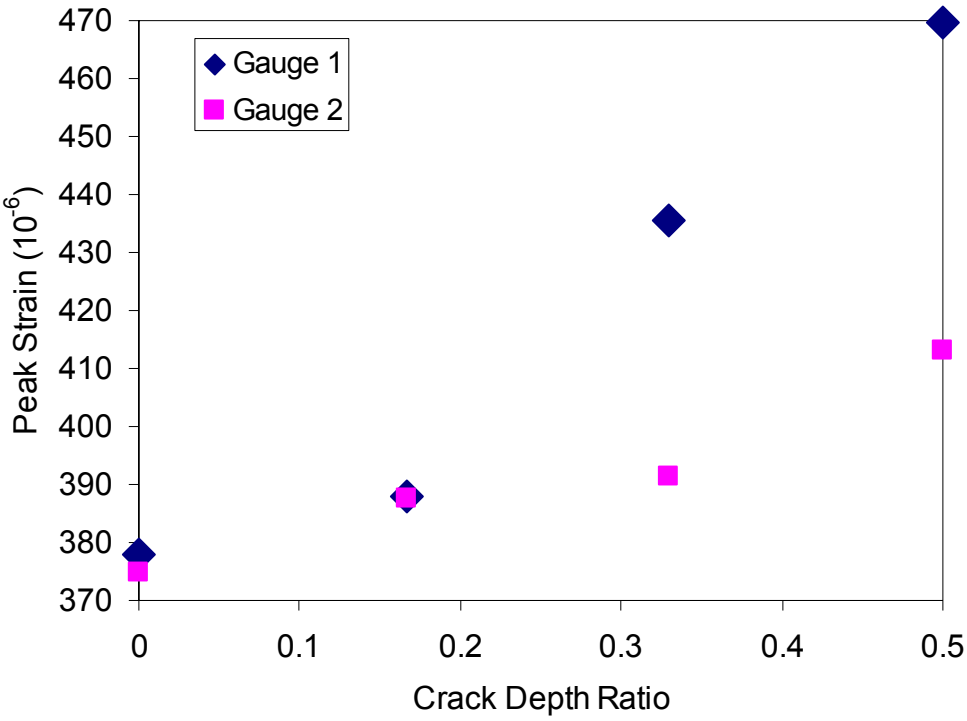

Figure 6a

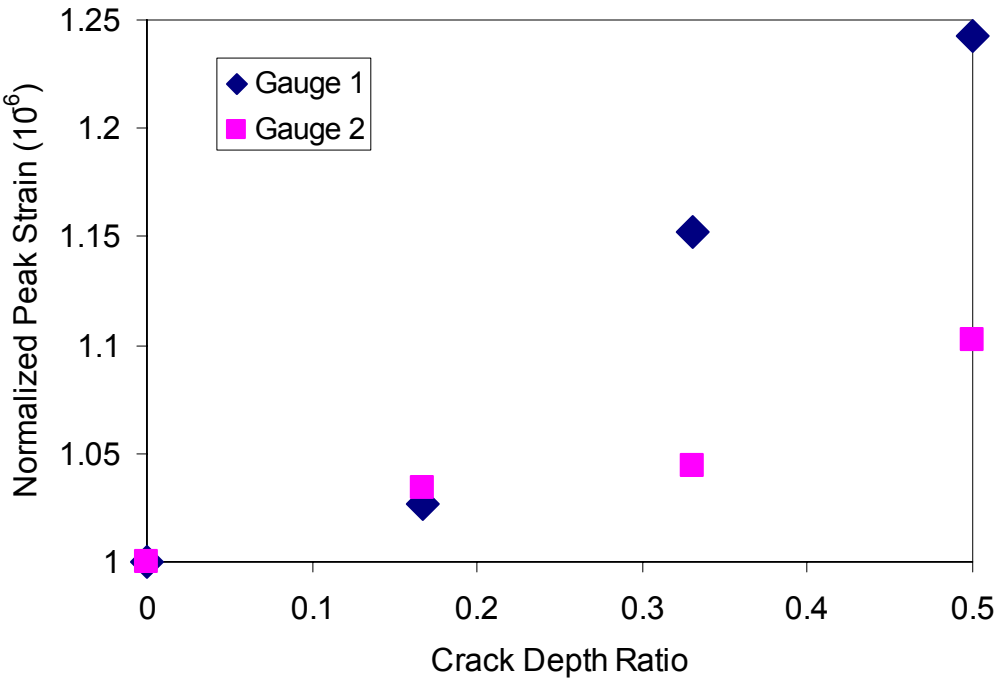

Figure 6b.

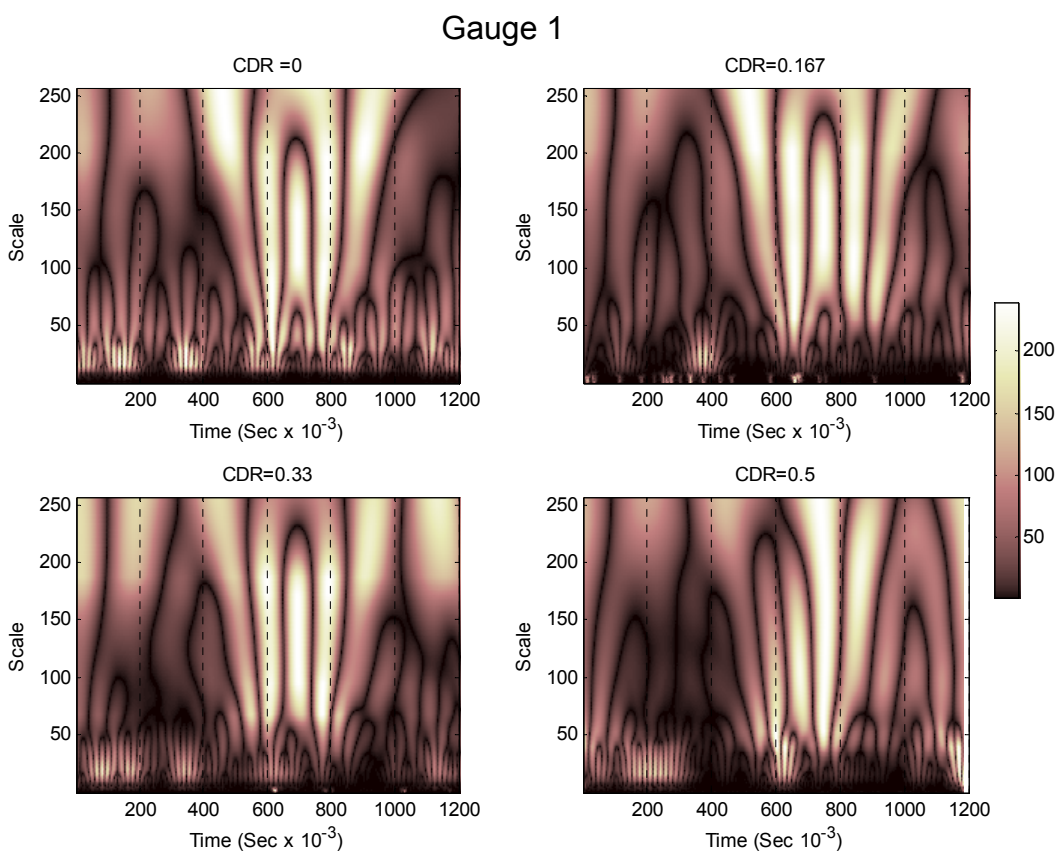
Gauge 1
CDR =0
CDR=0.167
CDR=0.33
CDR=0.5
Scale
Time (Sec x 10-3)
250
200
150
100
50
200
400
600
800
1000
1200

Figure 7a.

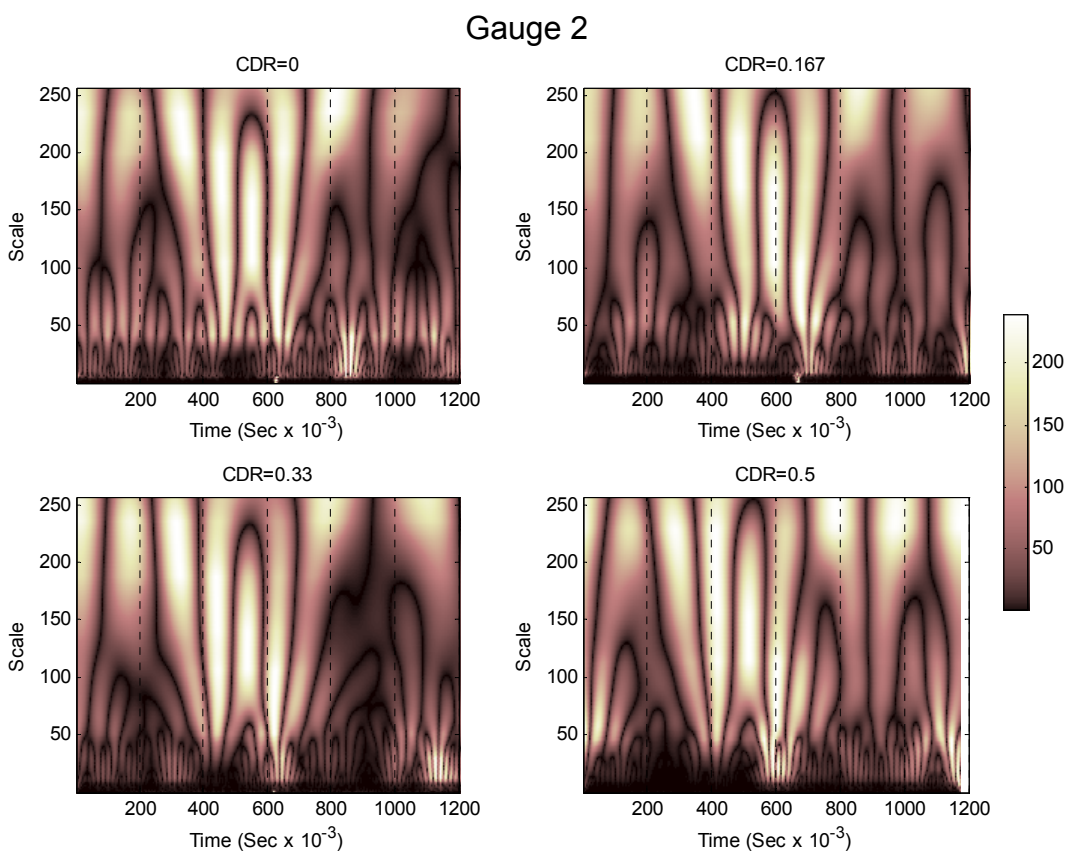
Gauge 2
CDR=0
CDR=0.167
CDR=0.33
CDR=0.5
Scale
Time (Sec x 10^-3)
250
200
150
100
50
200
400
600
800
1000
1200

Figure 7b.

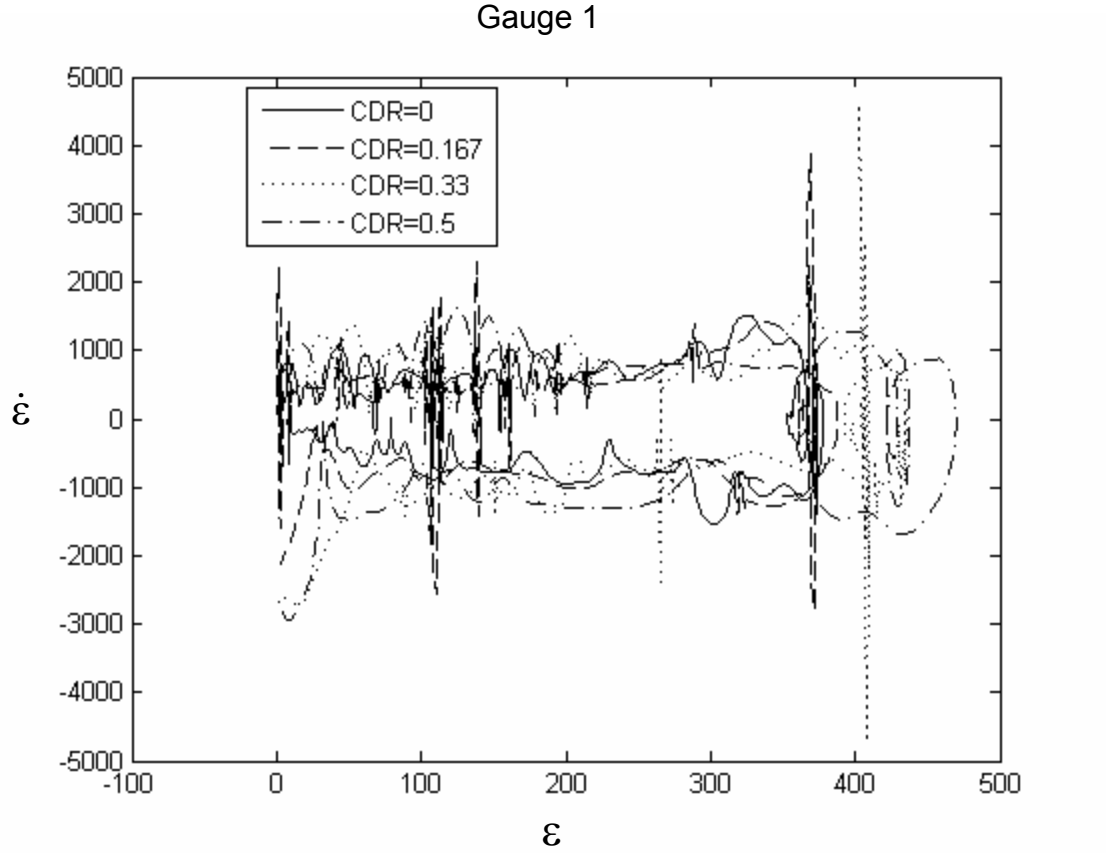
Gauge 1
CDR=0
CDR=0.167
CDR=0.33
CDR=0.5
5000
4000
3000
2000
1000
0
-1000
-2000
-3000
-4000
-5000
-100
0
100
200
300
400
500
ε̇
ε

Figure 8a.

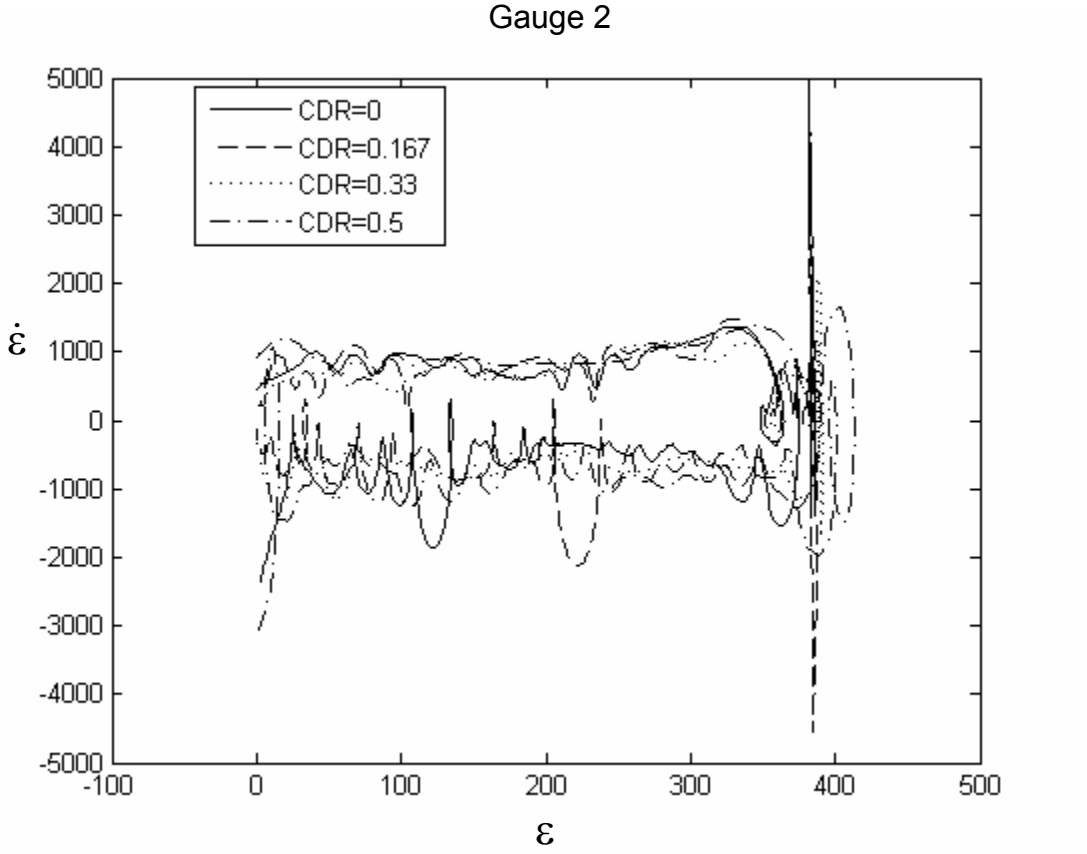
Gauge 2
CDR=0
CDR=0.167
CDR=0.33
CDR=0.5
5000
4000
3000
2000
1000
0
-1000
-2000
-3000
-4000
-5000
-100
0
100
200
300
400
500
ε̇
ε

Figure 8b.

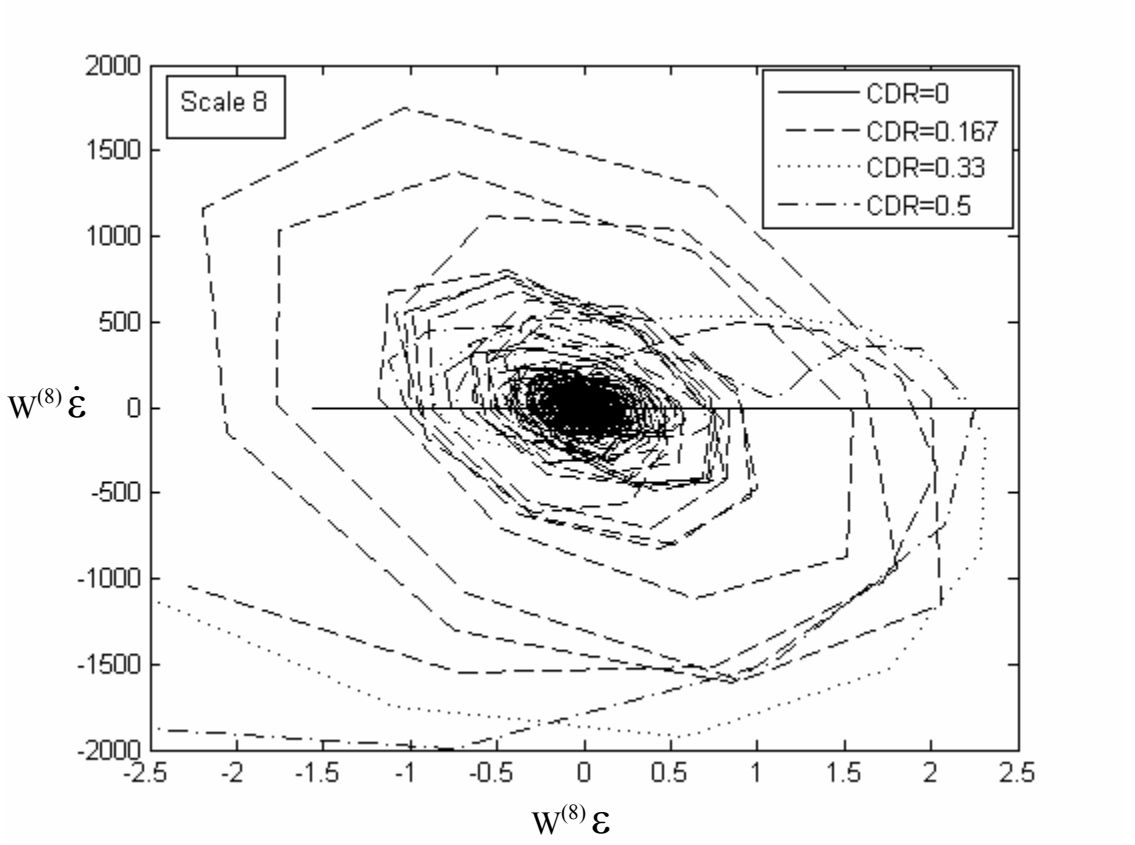
Scale 8
CDR=0
CDR=0.167
CDR=0.33
CDR=0.5
2000
1500
1000
500
0
-500
-1000
-1500
-2000
-2.5
-2
-1.5
-1
-0.5
0
0.5
1
1.5
2
2.5
$W^{(8)}\dot{\varepsilon}$
$W^{(8)}\varepsilon$

Figure 9a.

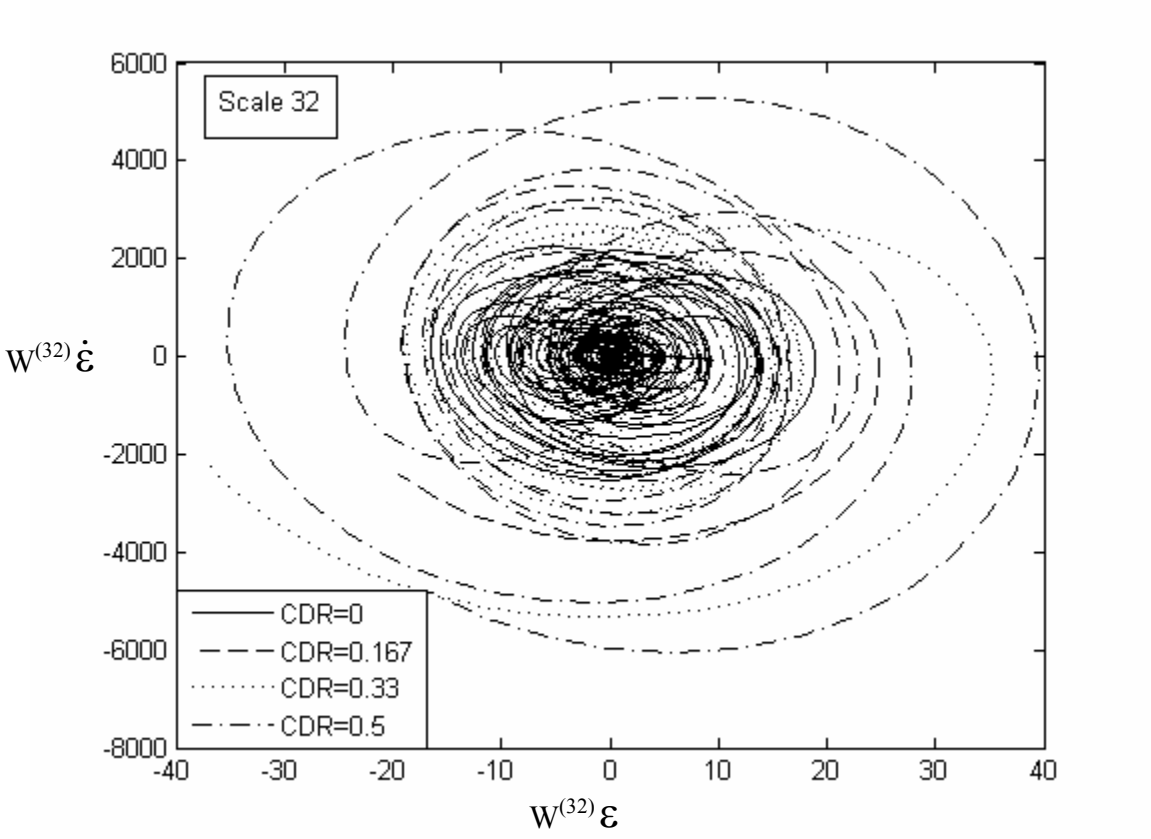
Scale 32
CDR=0
CDR=0.167
CDR=0.33
CDR=0.5
6000
4000
2000
0
-2000
-4000
-6000
-8000
-40
-30
-20
-10
0
10
20
30
40
W(32) ε̇
W(32) ε

Figure 9b.

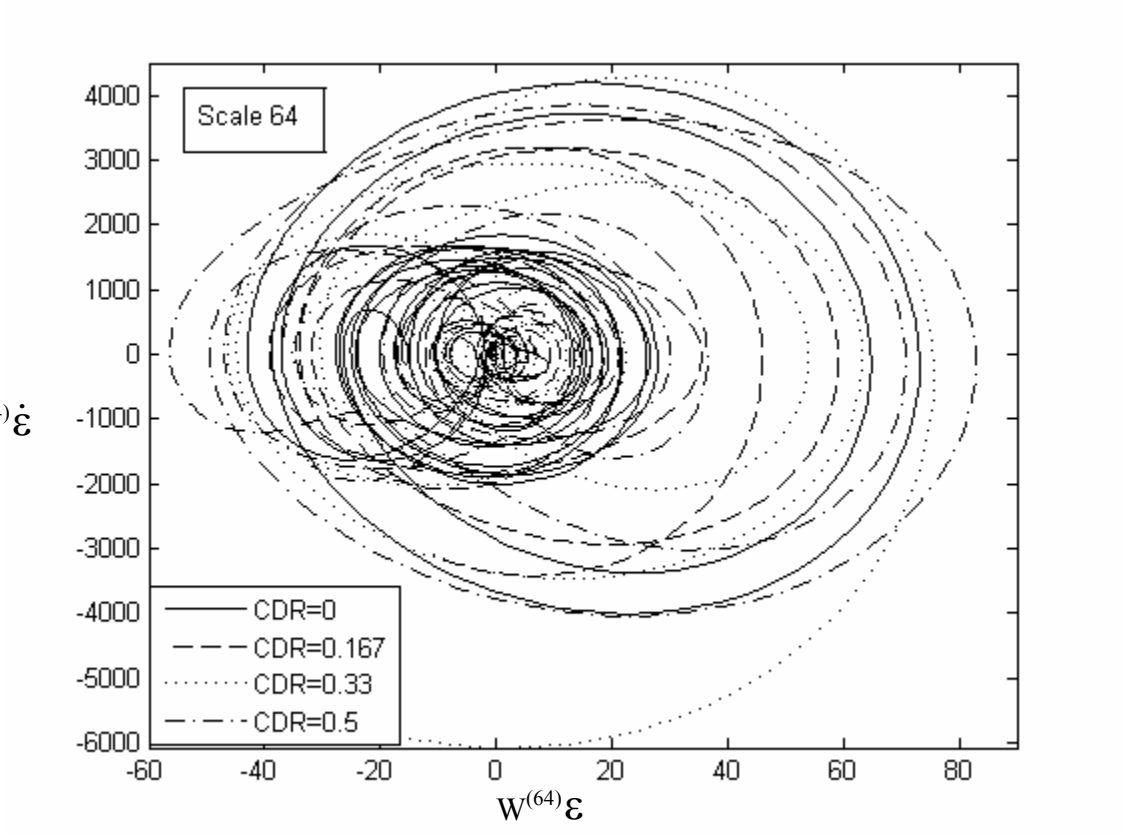
Scale 64
CDR=0
CDR=0.167
CDR=0.33
CDR=0.5
4000
3000
2000
1000
0
-1000
-2000
-3000
-4000
-5000
-6000
-60
-40
-20
0
20
40
60
80
$W^{(64)}\dot{\varepsilon}$
$W^{(64)}\varepsilon$

Figure 9c.

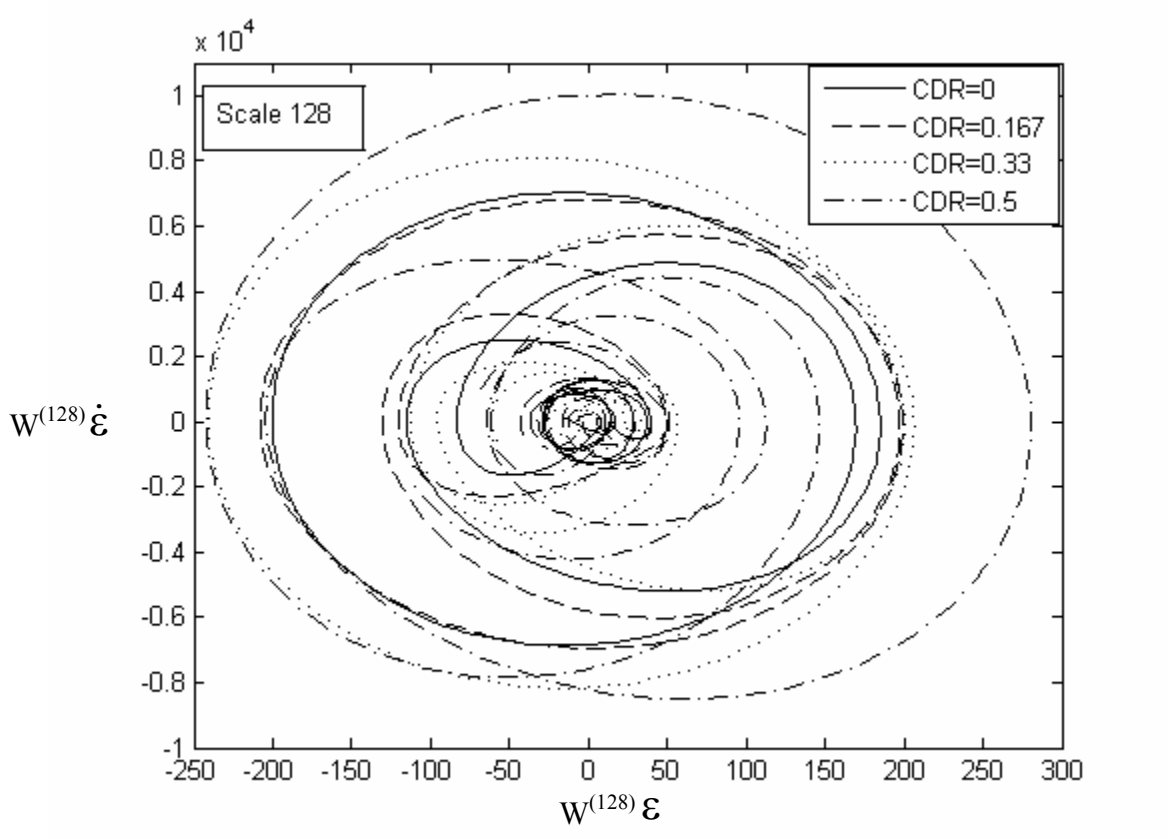
x 10^4
Scale 128
CDR=0
CDR=0.167
CDR=0.33
CDR=0.5
1
0.8
0.6
0.4
0.2
0
-0.2
-0.4
-0.6
-0.8
-1
-250
-200
-150
-100
-50
0
50
100
150
200
250
300
W(128) ε̇
W(128) ε

Figure 9d.

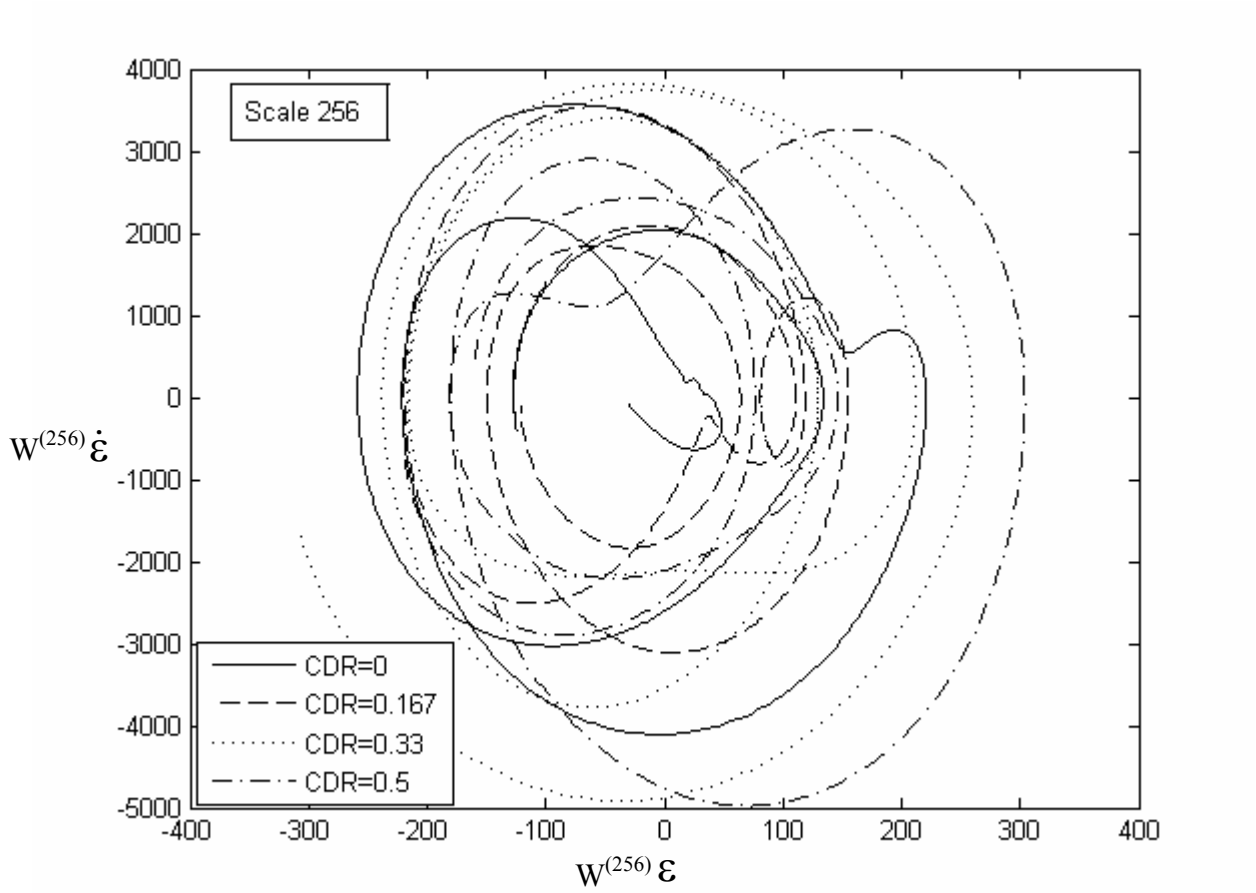
Scale 256
CDR=0
CDR=0.167
CDR=0.33
CDR=0.5
4000
3000
2000
1000
0
-1000
-2000
-3000
-4000
-5000
-400
-300
-200
-100
0
100
200
300
400
$W^{(256)}\dot{\varepsilon}$
$W^{(256)}\varepsilon$

Figure 9e.

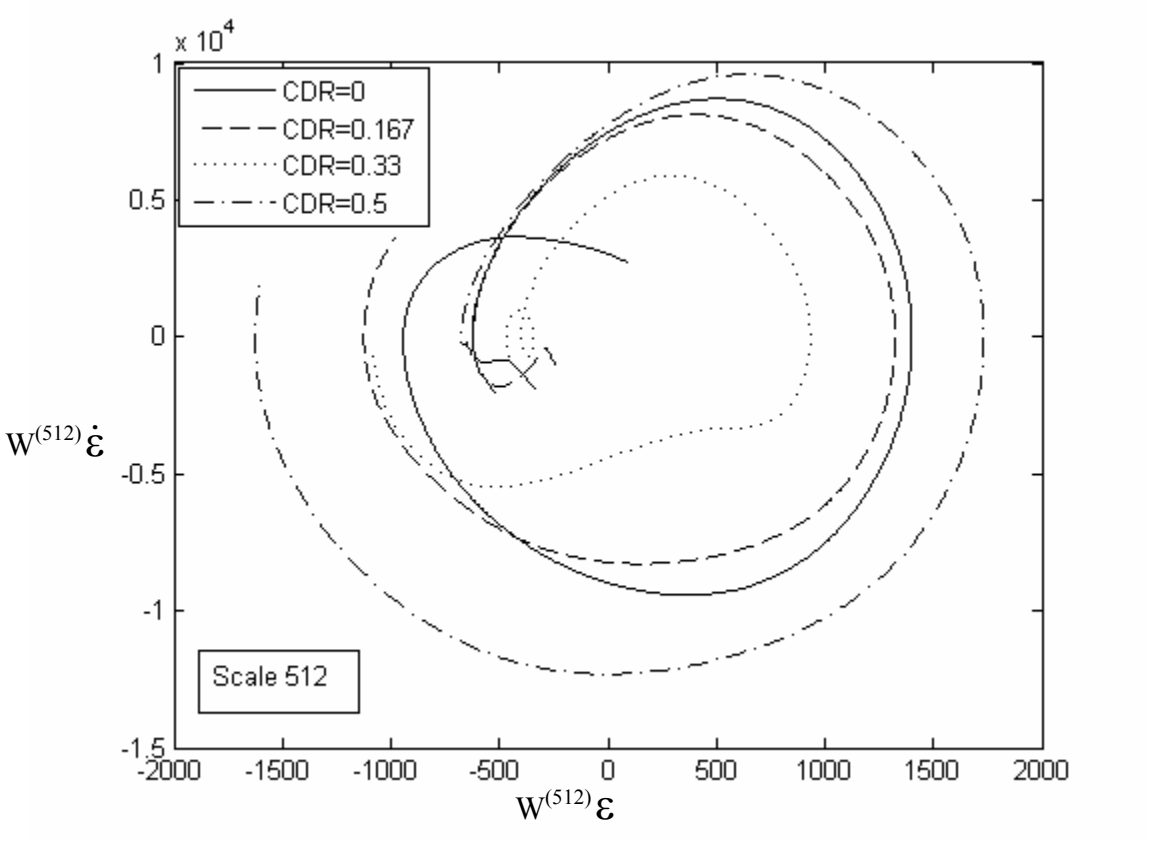
x 10^4
CDR=0
CDR=0.167
CDR=0.33
CDR=0.5
Scale 512
W(512) ε̇
W(512) ε
1
0.5
0
-0.5
-1
-1.5
-2000
-1500
-1000
-500
0
500
1000
1500
2000

Figure 9f.

Appendix 1. Matrix Representation of Equation 8

$$\begin{bmatrix} 1 & 0 & . & . & . & 0 \\ 0 & 1 & & & & \\ . & & . & & & \\ . & & & . & & \\ . & & & & . & \\ 0 & & & & & 1 \end{bmatrix}_{nxn} \begin{Bmatrix} \ddot{q}_1(t) \\ \ddot{q}_2(t) \\ . \\ . \\ . \\ \ddot{q}_n(t) \end{Bmatrix}_{nx1} + \begin{bmatrix} 2\xi_1\omega_1 & 0 & . & . & . & 0 \\ 0 & 2\xi_2\omega_2 & & & & \\ . & & . & & & \\ . & & & . & & \\ . & & & & . & \\ 0 & & & & & 2\xi_n\omega_n \end{bmatrix}_{nxn} \begin{Bmatrix} \dot{q}_1(t) \\ \dot{q}_2(t) \\ . \\ . \\ . \\ \dot{q}_n(t) \end{Bmatrix}_{nx1} + \begin{bmatrix} \omega_1^2 & 0 & . & . & . & 0 \\ 0 & \omega_2^2 & & & & \\ . & & . & & & \\ . & & & . & & \\ . & & & & . & \\ 0 & & & & & \omega_n^2 \end{bmatrix}_{nxn} \begin{Bmatrix} q_1(t) \\ q_2(t) \\ . \\ . \\ . \\ q_n(t) \end{Bmatrix}_{nx1} = \begin{Bmatrix} \sum_{j=1}^{\bar{n}} \frac{P_j}{\rho A \widehat{K}} \Phi_1 (u_0 t + \frac{1}{2} f t^2) \\ \sum_{j=1}^{\bar{n}} \frac{P_j}{\rho A \widehat{K}} \Phi_2 (u_0 t + \frac{1}{2} f t^2) \\ . \\ . \\ . \\ \sum_{j=1}^{\bar{n}} \frac{P_j}{\rho A \widehat{K}} \Phi_n (u_0 t + \frac{1}{2} f t^2) \end{Bmatrix}_{nx1}$$

where $\xi_{(.)}$ and $\omega_{(.)}$ are the damping ratios and the natural frequencies of the damaged beam respectively.